ULTRA-THIN ALD MGO MEMBRANES AS MEMS TRANSMISSION DYNODES IN A TIMED PHOTON COUNTER

Violeta Prodanovic[1,2], Hong Wah Chan[1,2], Anil U. Mane[3], Jeffrey W. Elam[3], Harry v.d. Graaf[1,2], and Pasqualina M. Sarro[1]

[1]Delft University of Technology, Else Kooi Laboratory, THE NETHERLANDS
[2]National Institute for Subatomic Physics, Amsterdam, THE NETHERLANDS
[3]Argonne National Laboratory, Argonne, USA

ABSTRACT

In this work we demonstrate how a novel single free electron detector "Timed Photon Counter" (TiPC) may benefit from ultra-thin MgO transmission dynodes (tynodes). These membranes are fabricated through MEMS process technologies, with atomic layer deposition (ALD) as the most apt technique for growing films of good quality, with excellent control over thicknesses and extremely low surface roughness. Large area arrays of ultra-thin (5 – 25 nm) free-standing MgO membranes are fabricated and characterized to determine the optimal thickness for application of ALD MgO in TiPC. Supremacy of MgO over other materials previously considered, such as SiN, Al_2O_3, SiC, Si is verified. The exceptional mechanical (low stress in particular, -200 MPa), chemical and electrical properties of MgO make this material a very attractive candidate for numerous MEMS applications, as the MEMS transmission dynodes in the timed photon counter.

INTRODUCTION

The Timed photon counter (TiPC) is a novel type of a photodetector, which has a working principle similar to photomultipliers. An essential part of this device is the tynode (transmission dynode), an array of freestanding membranes with thicknesses in the order of a few nanometers. After the impact of an incoming electron on one side of the tynode, noise-free amplification is provided through secondary electrons emission on the opposite side of the membrane. By vertical stacking of biased tynodes in vacuum and by placing them on top of a CMOS chip, an outstanding performance in terms of spatial and time resolution of this compact photodetector can be achieved (Fig. 1). Emission of electrons in transmission mode allows a significant reduction in size and weight of the device in comparison with existing photodetectors [1]. TiPC can be used in a wide range of detector applications, including solid state, atomic and molecular physics experiments, medical imaging, and commercial applications such as 3D optical imaging.

For proper operation, a tynode material must have satisfying transmission secondary electron yield (SEY). Insulating films are known to have a SEY higher than (semi)conductors, where generated electrons lose energy fast through scattering with conduction electrons and have small escape depths. Even so, an optimal electrical conductivity is required for replenishing the vacancies in the membrane after the escape of secondary electrons. To avoid charge-up effect, a very thin layer of conductive material is added on top of the membranes. From the point of view of fabrication, the tynode material must have such mechanical properties that freestanding membranes of only a few nanometers in thickness can be realized.

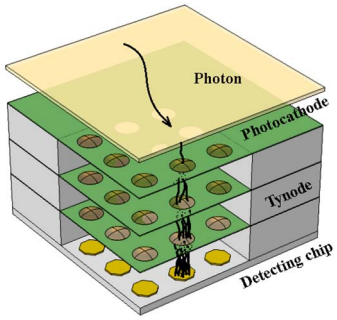

Figure 1: The essential part of a TiPC is a stack of tynodes placed on top of CMOS pixel chip. An avalanche of secondary electrons is created by biasing tynodes at different potentials. The number of required tynodes depends on the SEE of the applied emissive material.

Secondary electron emission (SEE) properties of a wide range of materials have been subject of extensive studies, but mostly on reflection SEY (RSEY) [2, 3]. It is reported that diamond with different surface terminations displays RSEY higher than 100 [4]. Excellent electron emission properties are also attributed to magnesium oxide, with RSEY in the 3.3 – 24.3 range [5], depending on growth method, surface composition and measurement approach. Numerous techniques have been employed for the deposition of MgO thin films, such as electron beam evaporation [6], chemical vapor deposition [7] and pulsed laser deposition [8]. For the growth of uniform very thin films on high aspect ratio structures, ALD is an ideal procedure as it enables a high control of the layer thickness by sequential self-limiting surface reactions at relatively low temperatures (down to 80°C, [9]). Different precursors have been employed in this process: β-diketonate and cyclopentadienyl-type gasses as metalorganic compounds and O_3, H_2O_2 or H_2O as oxidizers [10]. In addition, MgO is an attractive material due to its high melting point, wide band gap (7.8 eV) and low refractive index (1.73, as reported in this study). Regarding the application of MgO as a material with high SEE, ALD MgO proved to be an excellent choice for functionalization of large-area microchannel plates (MCP) detectors with a maximum measured RSEY of 6.9 after surface cleaning by ion sputtering [11].

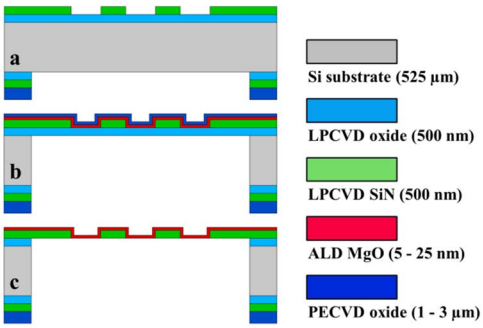

Figure 2: Process flow for fabrication of ALD MgO dynodes: the very thin ALD film is deposited on LPCVD SiN/oxide template (a) and protected additionally by thin oxide layer on top (b). After backside deep reactive ion etching of Si substrate oxide is gently removed by HF vapour to release the ultra-thin membranes sandwiched between LPCVD (bottom) and PECVD (top) oxide (c).

EXPERIMENTAL

Fabrication of tynodes

At first, several thicknesses were considered to determine the optimal value for the MgO membranes and to investigate its influence on the magnitude and energy position of SEY in the TiPC application. As substrate 4-inch Si <100> Si wafers, phosphorus-doped (5 – 10 Ωcm) and 525 ± 15 µm thick are used. An array of 64 x 64 free standing MgO membranes with thickness of 5, 15 and 25 nm, diameter of 10 – 30 µm and a center-to-center pitch of 55 µm is embedded in a 500nm thick LPCVD SiN and a 500nm thick thermal oxide mesh (Fig. 2a). The deposition parameters for the SiN are optimized to give a low-stress film. Growth is performed in a hot-wall reactor with values of temperature and gas pressure set to 850°C and 150 mTorr, respectively. Dichlorosilane (SiH_2Cl_2, DCS) is used as a source of silicon and ammonia (NH_3) as a source of nitrogen. After dry etching of wells in SiN, the wafers are ready for deposition of the tynode material. To ensure a safe release of the membranes, MgO is deposited on silicon oxide. Bis(cyclopentadienyl)magnesium ($Mg(Cp)_2$) and H_2O are used as reactants for synthesizing MgO films in a hot wall ALD reactor at 200°C. The $Mg(Cp)_2$ (purchased from Sigma-Aldrich) was maintained at 80°C, and deionized H_2O precursors at room temperature. Ultrahigh purity (99.999%) N_2 carrier gas flow was set to 300 sccm, providing a background pressure of 1.0 Torr in the reaction chamber as measured by a MKS Baratron pressure gauge. For the MgO ALD, the precursors $Mg(Cp)_2$ and H_2O were alternately pulsed in the continuous nitrogen carrier flow with the timing sequence: 3 s $Mg(Cp)_2$ dose – 15 s N_2 purge – 1 s H_2O dose – 15 s N_2 purge. To avoid formation of magnesium-hydroxide, exposure to the moist in the air is prevented by depositing 1 µm thick PECVD oxide on top (Fig 2b). In addition, this oxide layer provides a mechanical protection for MgO. DRIE is applied for the Si bulk etching from the wafer backside, and final release of membrane arrays is then achieved by utilizing HF vapour with a flow of 190 sccm at 125 Torr (Fig 2c). The survival rate of the membranes is larger than 97%, and no significant surface distortion of their surface is observed (Fig 3). To supress charging up of the membranes, which influences the precision of SEY measurements, a very thin conductive layer is applied on top of the SEE material. In this experiment a 1.8 – 2 nm thin TiN layer is sputtered on the MgO membranes prior to the SEY measurement.

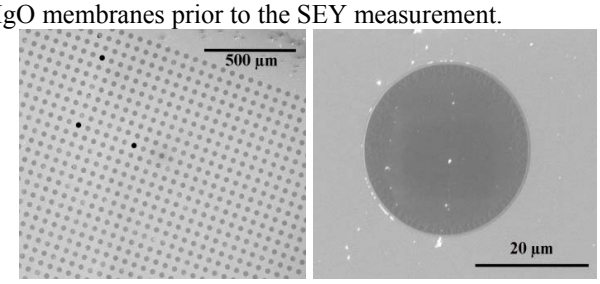

Figure 3: SEM captures of 5 nm thin MgO membranes in 64 x 64 array with a center-to-center distance of 55 µm. Most dynodes remained intact after release, with only couple of ruptured membranes (black spots on left image).

The structural, mechanical and optical properties of the ALD thin films are characterized. MgO layer thickness is measured on blank wafers by spectroscopic ellipsometry acquired at four different angles between 50° and 65°. The Cauchy dispersion model is applied to determine optical coefficients for somewhat thicker MgO films (around 50 nm) and this fixed set of data is then used afterwards to fit the thin layers measurements. X-ray photoelectron spectroscopy (XPS) is employed for composition analysis. Wide scans were acquired using 200 eV analyzer pass energy and a 1 eV step and high resolution spectra of the C 1s, Mg 2p and O 1s regions were recorded using 50 eV pass energy and 0.1 eV steps. The crystalline orientation of the films is examined by recording X-ray diffraction (XRD) graphs by Bruker D8 Advance diffractometer using Cu-Kα radiation at 45 kV and 40 mA. Diffraction patterns were recorded for the angle of incidence (2θ) in the range 20° - 65°, with a step size 0.034° and step time of 10 s. Data evaluation is then performed with Bruker Software DiffracSuite.EVA. Information on surface morphology data is obtained by atomic force microscopy (AFM) in a non-contact mode with a silicon tip (radius 5 nm), over 0.5 x 0.5 μm^2 area. Stress of MgO films is calculated by recording curvature of a wafer in a laser-based system prior to and after deposition of MgO.

Dual Faraday Cup

The Dual Faraday Cup (DFC) is a setup used to determine the SEY of tynodes inside a SEM (FEI NovaNanoLab 650 Dual Beam). For transmission measurements, the setup consists of a sample holder, retarding grid and a collector and is mounted onto the stage of the SEM, with typical operating vacuum level of 10^{-5} – 10^{-6} mbar. The electrodes are electrically insulated from each other by means of polyiamide foil and are connected to

a Keithley 2450 source meter via a vacuum feed through. The meter allows the electrodes to be biased from -200 V up to +200 V, while simultaneously measuring the current. The electron gun of the SEM has an energy range from 300 eV up to 30 keV. For the transmission measurement presented here, a 2 x 2 cm^2 chip with MgO tynode is clamped inside the holder and is biased at -50 V, while the retarding grid and the collector are held at ground potential. The negative bias repels the escaped electrons from the sample surface towards the retarding grid and collector. The transmitted electrons consist of transmission secondary electrons (< 50 eV) and forward scattered electrons (> 50 eV) and are not distinguished here. The averaged current density depends on the chosen magnification. The used primary electron beam current is between 50 pA and 0.5 nA depending on the electron energy.

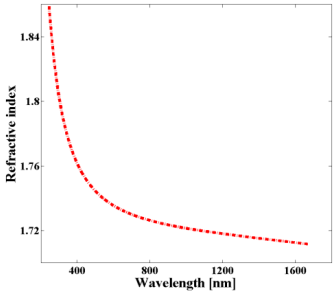

Figure 4: Refractive index of ALD MgO measured on 25 nm thin film. Its value at 633 nm is 1.73.

RESULTS AND DISCUSSION

Material characterization

The layer uniformity is evaluated by ellipsometry considering 13 data points across the wafer. The thickness of MgO on Si substrate is 25.53 ± 0.41 nm, with an estimated growth per cycle of 0.165 nm. The plot of refractive index versus wavelength for this film is given in Fig. 4. In XPS analysis of as-deposited MgO films only magnesium, oxide and carbon peaks are detectable, as expected. Additional XPS survey with ion milling reveals that carbon is present only as surface contamination and is not incorporated in the layer during the deposition process. Similar to the study reported in [11], a smaller peak next to O 1s binding energy is observed and can be attributed to adsorption of OH groups. The Mg:O atomic ratio of 1.034 implies a good stoichiometry of the investigated film. X-ray scattering from 25 nm MgO on top of (100) Si substrate is presented in Fig. 6, after background subtraction. The colored lines stand for the peak positions and intensities of possibly present crystalline phases. The broad feature between 20° and 35° on the 2θ-axis in the plotted graph suggests that the major part of the film is amorphous. The stress of 50 nm ALD MgO is compressive and calculated to be around 200 MPa. RMS obtained from AFM data is around 0.4 nm (Fig. 7), which is lower than reported results [9, 12].

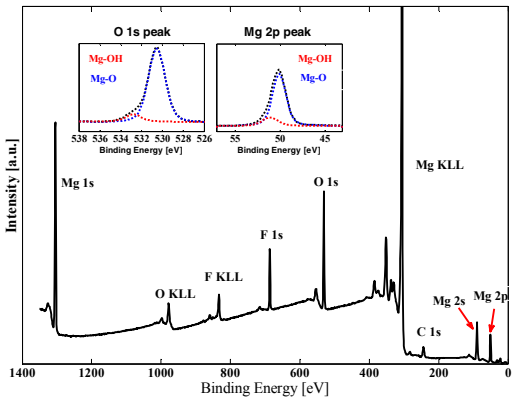

Figure 5: XPS spectra of 25 nm ALD MgO after HF etching. Observed carbon originates from a surface contamination and F peaks probably occur due to HF vapour etching.

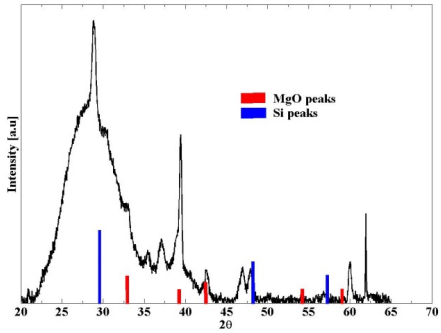

Figure 6: X-ray diffraction diagram of 25 nm MgO film deposited at 200°C on Si substrate. No ordered crystalline structure is observed for these growth conditions.

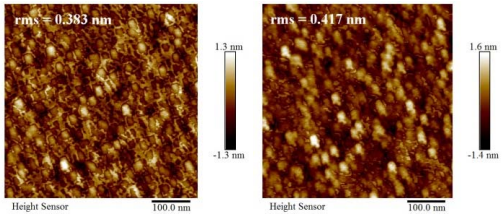

Figure 7: AFM image of released 25 nm thin MgO membrane (left) and on the substrate next to the membrane (right). Size of scanned area is 0.5 x 0.5 μm^2.

Transmission SEE.

TSEY of MgO tynodes of three thicknesses (5, 15 and 25 nm) is investigated. After data collection, a dependency of TSEY over thickness is plotted in Fig. 8. The 5 nm thin MgO membranes have TSEY of almost 3, significantly higher than other materials we previously considered, such as SiN, SiC and Si, as well as compared to what achieved with ALD Al_2O_3 (Fig. 9), which was the best candidate for TiPC application investigated so far, with a TSEY of 2.6 for 10 nm thin membranes. This optimal tynode thickness is expected to be in the range of the escape depth of the material [6]. Decreasing the thickness of the tynode below the escape depth of the material will reduce the maximum TSEY since the interaction volume with the primary

electron beam decreases. Charge-up effects were observed after prolonged irradiation of the surface. Therefore, each data point is collected from a different membrane inside the array when the electron energy is increased. Due to such recording the electron yield curve is not as smooth as the measurement of a single large Al_2O_3 membranes.

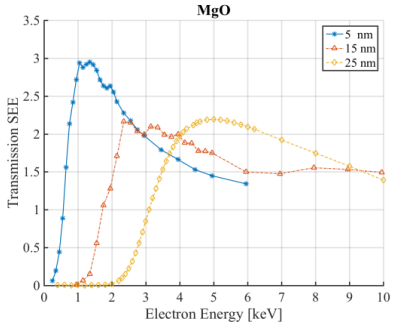

Figure 8: Transmission SEE of ALD MgO membranes with different thicknesses versus energy of incoming electrons.

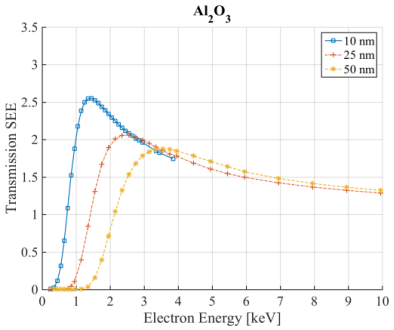

Figure 9: Transmission SEE of ALD Al_2O_3 membranes, 10 to 50 nm thin. This material does not exhibit such a high yield as the investigated MgO.

Conclusions and future work

Large area arrays of ultra-thin (5-25 nm) free-standing MgO membranes are successfully fabricated and characterized. The optimal film thickness for the secondary emissive ALD MgO membranes was found to be 5 nm. ALD provides a superior and simple way to ensure thickness and conformality control, which is necessary for a reliable production process of smooth ultra-thin membranes. We demonstrated that for TiPC application MgO is better suited than alumina due to its increased TSEY. Performance of MgO membranes can be further improved by lowering electron affinity through a convenient surface termination. Effects of surface cleanliness, aging of material and crystallization of material by thermal bake out remain to be investigated. The exceptional mechanical, chemical and electrical properties of MgO make this material a very attractive candidate for numerous MEMS applications, such as a masking layer for DRIE and HF etching, gate oxide, passivating film in optical materials and barrier layer in tunnel junctions.

ACKNOWLEDGEMENTS

This work is a part of MEMBrane project supported by European Research Council. Authors wish to thank all collaborators at Else Kooi Laboratory, Brookhaven National Lab, Argonne National Lab, ImPhys group at Faculty of Applied Sciences (TU Delft), especially M. Kamerbeek, R. Hendrikx and C. Helvoirt for help with various measurements of MgO.

REFERENCES

[1] H. v. d. Graaf, M. Bakker, H. Chan, E. Charbon, F. Santagata, P. M. Sarro, "The Tipsy single photon detector and Trixy ultrafast tracking detector", *JINST*, 8, C01306, 2013.

[2] J. Cazaux, "E-induced secondary electron emission yield of insulators and charging effects", *Nucl. Instr. and Methods in Phys. Research,* 244(2), pp. 307–322, 2006.

[3] J. Barnard, I. Bojko, N. Hilleret, "Measurements of the secondary electron emission of some insulators", *LHC-VAC/Io.B*, 1997.

[4] J. E. Yater, A. Shih, "Secondary electron emission characteristics of single-crystal and polycrystalline diamond", *J. Appl. Phys*., 87, 2000, pp. 8103-8112, 2000.

[5] Y. Ushio, T. Banno, N. Matuda, S. Baba, A. Kinbara "Secondary electron emission studies on MgO films", *Thin Solid Film*, 167, pp. 299-308, 1988.

[6] N. R. Rajopadhye, V. A. Joglekar, V. N. Bhoraskar, S. V. Bhoraskar, "Ion secondary electron emission from Al_2O_3 and MgO films", *Solid State Commun.*, 60, pp. 675-679, 1986.

[7] E. Fujii, A. Tomozawa, H. Torii, R. Takayama, M. Nagaki, T. Narusawa, "Preferred orientations and microstructure of MgO films prepared by plasma-enhanced metalorganic chemical vapor deposition", *Thin Solid Films*, 352, pp. 85-90, 1999.

[8] X. Y. Chen, K. H. Wong, C. L. Mak, X. B. Yin, M. Wang, J. M. Liu, Z. G. Liu, "Selective growth of (100)-, (110)-, and (111)-oriented MgO films on Si(100) by pulsed laser deposition", *J. Appl. Phys*., 91, pp. 5728-5734, 2002.

[9] S. Vangelista, R. Mantovan, A. Lamperti, G. Tallarida, B. Kutrzeba-Kotowska, S. Spiga, M. Fanciulli, "Low-temperature atomic layer deposition of MgO thin films on Si", J. Phys. D: Appl. Phys, 46, 485304, 2013.

[10] M. Putkonen, L. Johansson, E. Rauhala, L.Niinisto, "Surface-controlled growth of magnesium oxide thin films by atomic layer epitaxy", *J. Mater. Chem*., 9, pp. 2449-2452, 1999.

[11] S. J. Jokela, I. V. Veryovkin, A. V. Zinovev, J. W. Elam, A. U. Mane, Q. Peng, Z. Insepov, "Secondary electron yield of emissive materials for large-area micro-channel plate detectors: surface composition and film thickness dependencies", *Physics Procedia*, 37, pp. 740-747, 2012.

[12] M. Putkonen, T. Sajavaara, L. Niinisto, "Enhanced growth rate in atomic layer epitaxy deposition of magnesium oxide thin films", J. Mater. Chem., 10, pp. 1857-1861, 2000.